Design of an Automated Thermal Cycler for Long-term Phase Change Material Phase Transition Stability Studies

A. C. Kheirabadi, D. Groulx*
Laboratory of Applied Multiphase Thermal Engineering (LAMTE), Dalhousie University
*Corresponding author: 5269 Morris Street – room C304, Halifax NS Canada B3H 4R2, dominic.groulx@dal.ca

Abstract: This paper highlights the use of COMSOL Multiphysics during the design process of a thermal cycling system for regulated PCM phase transitioning. The primary purpose of the conducted simulations was to predict the system behavior in response to an ON/OFF temperature control system prior to commencing the construction process.

The simulation results indicated that the system temperature was controllable within a practical timeframe through cartridge heaters (as heating mechanisms) and thermoelectric Peltier modules (as cooling mechanisms). Additionally, the results indicated that a complete phase change cycle (melting and solidification) was achievable within 16 minutes for PCMs with melting temperatures between 30 °C and 60 °C.

Upon construction of the thermal cycling system, simulation results were validated against experimentally collected data. Good correlations were identified for the system temperature response to the implemented heating and cooling control systems. Good correlations were also identified for PCM behavior during solidification.

Keywords: Heat Transfer, Phase Change Materials, Temperature Control System, Peltier (Thermoelectric) Modules

1. Introduction

Phase change materials (PCMs) are capable of storing and releasing large amounts of thermal energy when transitioning between solid and liquid phases, a characteristic that has major implications in thermal energy storage systems [1]. This is due to the high latent heat of fusion required for a PCM to fully melt or solidify.

When subject to long-term use however, questions are raised regarding the performance of PCMs after a large number of phase transition cycles have occurred. Consequently, the design of an automated thermal cycling system was undertaken to allow for frequent, long-term phase transition cycling of PCM samples for experimental analysis.

COMSOL Multiphysics was used to predict the system behavior in response to an ON/OFF temperature control system prior to construction. Items of interest included the dynamic behavior of the heating and cooling devices, as well as the time required for complete phase change of PCM samples.

This paper presents the methods and parameters used in COMSOL simulations, followed by a comparison between numerical and experimental results for validation.

2. Thermal Cycler Design

2.1 Block Housing

The thermal cycler to be designed is shown in Fig. 1. The system consists of an aluminum block that houses eight dram vials containing PCM samples, two cartridge heaters, a negative coefficient (NTC) thermistor, and four thermoelectric cooling subassemblies.

2.2 Heating Subsystem

The system is heated through two high temperature cartridge heaters inserted into separate slots within the aluminum housing. As shown in Fig. 2, each cluster of four dram vials surrounds one cartridge heater. The probed element at the center of the housing is the NTC thermistor.

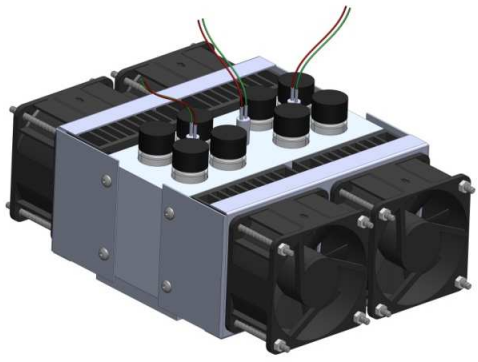

Figure 1 – Thermal cycling system

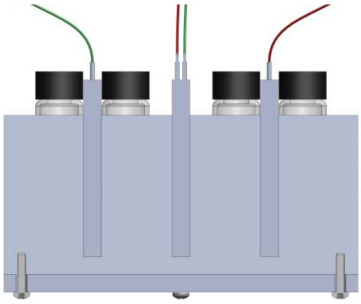

Figure 2 – Cross sectional view of the block housing

2.3 Cooling Subsystem

The block housing is cooled through four thermoelectric cooling subassemblies; each containing a TE Technology Peltier module, an aluminum heat sink, and a cooling fan. As shown in Fig. 3, each heat sink is bolted directly onto the side walls of the aluminum housing with a Peltier module compressed in-between. The cooling fans are maintained directly above each heat sink through custom-made mounting brackets.

Heat transfer through a single cooling subassembly is visualized in Fig. 4. Heat is removed from the aluminum housing and stored within the adjacent heat sinks; this heat transfer is induced by the temperature difference generated across the Peltier modules. Heat is then dissipated from the heat sink fins to the surrounding air through forced convection induced by the cooling fans.

2.4 Temperature Control System

The aluminum housing temperature is regulated by an ON/OFF control system that performs logical operations based on feedback from the NTC thermistor. The heating/cooling subsystems are actuated such that the housing temperature is maintained within a desired range.

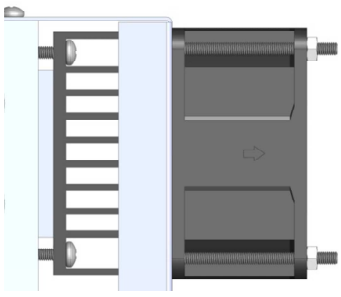

Figure 3 – Top view of a single thermoelectric cooling subassembly

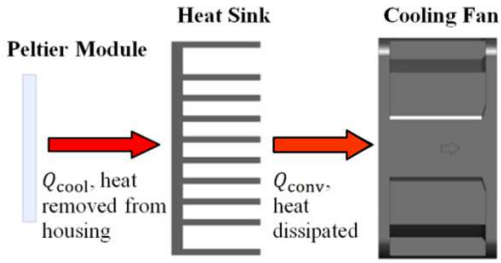

Figure 4 – Heat transfer through thermoelectric cooling assembly

Table 1 – PCM properties [5]

Property	Eicosane	Docosane	Myristic Acid
C_s (J/kg·K)	1715	1800	2000
C_l (J/kg·K)	2267	2320	2670
k_s (W/m·K)	0.25	0.25	0.20
k_l (W/m·K)	0.15	0.15	0.16
ΔH_f (kJ/kg)	237	253	198
ρ_{T_m} (kg/m^3)	776	781	860
ΔT (K)	10	10	10
α (J/kg·K)	59380	63670	46105
β (1/K^2)	0.2348	0.2355	0.2185

2.5 Phase Change Materials for Validation

Melting and solidification was simulated for three different PCM samples; eicosane, docosane, and myristic acid (tetradecanoic acid). The properties and phase change parameters of these PCMs are listed in Table 1.

3. Use of COMSOL Multiphysics

3.1 Geometry

The 3D COMSOL model, shown in Fig. 5, is an eighth cutout of the complete cycling system. It contains a single dram vial of PCM surrounded by a section of aluminum, a half cutout of a single heat sink, and a quarter section of the cartridge heater contact face. A sample of PCM rests at the bottom of the dram vial, while the remaining volume is filled with air domains. The relevant dimensions of the COMSOL model are shown in Fig. 6 and are listed in Table 2.

3.2 Finite Element Mesh

The finite element mesh, also shown in Fig.5, consists of free tetrahedral elements with properties listed in Table 3. These properties are the result of a mesh convergence study.

3.3 COMSOL Physics Nodes

Heat Transfer in Solids was the only COMSOL physics node used for simulation. In order to model complex behaviors found in

phase change and thermoelectric cooling, approximation methods were identified and were later validated against experimental data. These methods are presented in the following subsections.

Table 2 – COMSOL model dimensions

Dimension	Value
H_{block}	2.500 in
L_{block}	1.170 in
H_{air}	1.937 in
H_{PCM}	0.335 in
D_{vial}	0.680 in
t_{TEC}	0.142 in
L_{TEC}	1.575 in
$A_{\text{TEC}} = {L_{\text{TEC}}}^2/2$	1.240 in^2

Table 3 – Finite element mesh properties

Property	Value
Max. Element Size	0.112 in
Min. Element Size	0.00478 in
Growth Rate	1.35
Curv. Factor	0.3
Narrow Res.	0.85
No. Elements	106,318

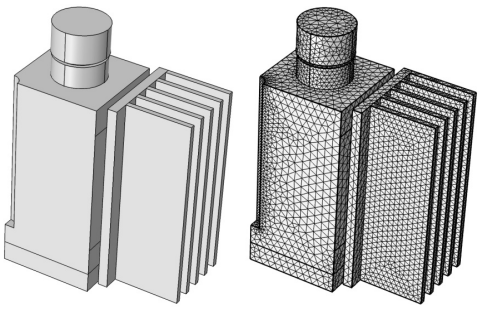

Figure 5 – 3D COMSOL geometry and mesh

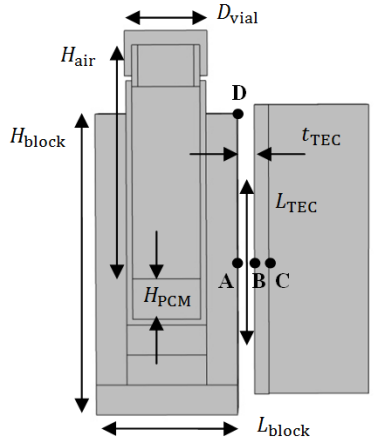

Figure 6 – COMSOL model dimensions

3.4 Simulating Phase Change

At the phase transition temperature, the specific heat capacity of a material resembles a Dirac delta function. This behavior was approximated in COMSOL by adding a continuous function, shown in Fig. 7, in place of the PCM specific heat capacity. This function consists of a sigmoid function representing the heat capacity transition from solid to liquid form, as well as a Gaussian function representing the increase in heat capacity during phase change.

The primary condition is that the integral of the specific heat capacity between T_1 and T_2 is equal to the sum of the latent heat of fusion and sensible heat of the material in question. Additionally, the specific heat capacities before and after the integrated region must represent the specific heat capacities of the material in solid and liquid form, respectively.

The resulting specific heat capacity of a material experiencing phase change was modeled through Eq. (1).

$$C_{\text{p}} = C_{\text{s}} + \frac{C_{\text{l}} - C_{\text{s}}}{1+\text{e}^{-r(T-T_{\text{m}})}} + \alpha \text{e}^{-\beta(T-T_{\text{m}})^2} \quad (1)$$

C_{s} and C_{l} are the material specific heat capacities in solid and liquid form, respectively, T is the material temperature solved locally within COMSOL, T_{m} is the material melting temperature, and ΔT is the width of the integrated region (*i.e.* T_2 minus T_1). α and β are determined numerically to satisfy the integral requirement, and r is calculated according to Eq. (2).

$$r = \frac{10}{\Delta T} \quad (2)$$

The thermal conductivity of a material experiencing phase change simply transitions from one value to another at the melting temperature. This was modeled through a sigmoid function as shown in Eq. (3).

$$k = k_{\text{s}} - \frac{k_{\text{s}} - k_{\text{l}}}{1+\text{e}^{-r(T-T_{\text{m}})}} \quad (3)$$

k_{s} and k_{l} are the thermal conductivities in solid and liquid form, respectively. The density of the PCM was held constant and set equal to its density at the melting temperature, $\rho_{T_{\text{m}}}$.

3.5 Simulating Cartridge Heaters

When active, the cartridge heater supplies a constant heat rate, Q_{CH}, into the system. The

ON/OFF status of the heating control system was modeled through Eq. (4).

$$X_{\text{heat}} = (T_{\text{Al}} < T_{\text{heat}} - T_{\text{f}}) + (T_{\text{Al}} > T_{\text{heat}} - T_{\text{f}}) \cdot (T_{\text{Al}} < T_{\text{heat}}) \cdot \left(\frac{\mathrm{d}T_{\text{Al}}}{\mathrm{d}t} > 0\right) \quad (4)$$

X_{heat} is a 1 or 0 multiplier that determines the ON/OFF status of the control system, T_{Al} is the aluminum housing temperature derived within COMSOL through a domain point probe (located at point D in Fig. 6), T_{heat} is the desired hot temperature, and T_{f} is the allowable fluctuation from the desired temperature which defines the desired temperature range.

If T_{Al} is below the desired temperature range, the heater is actuated. If T_{Al} approaches the desired temperature range from below (while heating), the heater remains actuated until T_{Al} exceeds T_{heat}. If T_{Al} approaches the desired temperature range from above (heating is off), the heater remains deactivated until T_{Al} is again below the desired temperature range.

The control system during the heating phase was then modeled by adding Eq. (5) as an expression for the heat flux on the cartridge heater contact face.

$$Q_{\text{heat}} = X_{\text{heat}} \cdot Q_{\text{CH}} \quad (5)$$

3.6 Simulating Peltier Modules

The dynamics of Peltier modules are dependent upon the DC voltage across the module terminals, as well as the hot and cold side temperatures of the module. Manufacturers of Peltier modules typically provide information relating the cooling rate to the voltage, hot side temperature, and temperature difference across the module. A performance graph of the Peltier modules used was provided by TE Technology and is shown in Fig. 8.

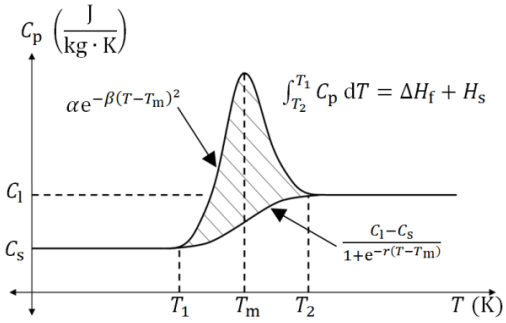

Figure 7 – Specific heat capacity approximation for phase change simulation

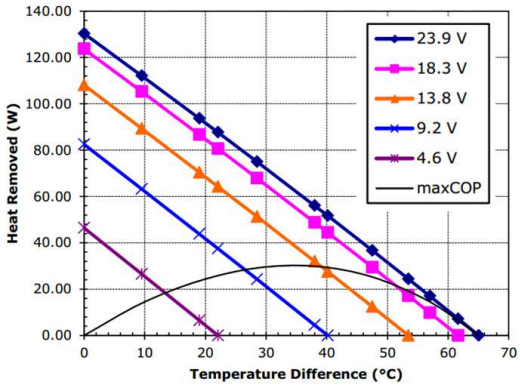

Figure 8 – Peltier module cooling rate at a hot side temperature of 30 °C [2]

Such graphs were provided for hot side temperatures of 30, 50, and 70 °C. Therefore interpolation was used to predict the behavior of Peltier modules at any other hot side temperature.

The total cooling rate available to the system as a function of DC voltage and the temperature difference across the Peltier module is calculated according to Eq. (6). This is simply the equation of a sloped line from Fig. 8.

$$Q_{\text{TEC}} = \frac{1}{2} Q_{\text{max}} \left(1 - \frac{\Delta T_{\text{TEC}}}{\Delta T_{\text{max}}}\right) \quad (6)$$

ΔT_{TEC} is the instantaneous temperature difference across the Peltier modules (*i.e.* hot side minus cold side) derived within COMSOL through domain point probes (located at points A and B in Fig. 6, respectively), and Q_{max} and ΔT_{max} are the maximum cooling rate and temperature difference across the modules as defined in Eqs. (7) and (8).

$$Q_{\text{max}} = \alpha_{\text{Q}} T_{\text{H}} + \beta_{\text{Q}} \quad (7)$$

$$\Delta T_{\text{max}} = \alpha_{\text{T}} T_{\text{H}} + \beta_{\text{T}} \quad (8)$$

T_H is the hot side temperature of the Peltier modules derived within COMSOL through a domain point probe (located at point B in Fig. 6), and α_{Q}, α_{T}, β_{Q}, and β_{T} are interpolation parameters defined in Eqs. (9) through (12).

$$\alpha_{\text{Q}} = \frac{Q_{\text{max@70 °C}} - Q_{\text{max@30 °C}}}{40\ °\text{C}} \quad (9)$$

$$\alpha_{\text{T}} = \frac{\Delta T_{\text{max@70 °C}} - \Delta T_{\text{max@30 °C}}}{40\ °\text{C}} \quad (10)$$

$$\beta_{\text{Q}} = Q_{\text{max@70 °C}} - \alpha_{\text{Q}}(70\ °\text{C} + 273.15\ °\text{C}) \quad (11)$$

$$\beta_{\text{T}} = \Delta T_{\text{max@70 °C}} - \alpha_{\text{T}}(70\ °\text{C} + 273.15\ °\text{C}) \quad (12)$$

$Q_{\max_{@30\,°C}}$, $Q_{\max_{@70\,°C}}$, $\Delta T_{\max_{@30\,°C}}$, and $\Delta T_{\max_{@70\,°C}}$ were derived based on polynomial regressions of performance data provided by the Peltier module manufacturer. These second order regressions are listed in Eqs. (13) through (16).

$$Q_{\max_{@30\,°C}} = -0.2372V^2 + 11.118V - 0.1608 \quad (13)$$

$$Q_{\max_{@70\,°C}} = -0.1544V^2 + 9.1577V + 17.558 \quad (14)$$

$$\Delta T_{\max_{@30\,°C}} = -0.1163V^2 + 5.5563V - 1.1939 \quad (15)$$

$$\Delta T_{\max_{@70\,°C}} = -0.1012V^2 + 5.6852V - 0.8129 \quad (16)$$

V is the DC voltage across the Peltier modules; this value is constant throughout the simulations. The ON/OFF controller was then modeled according to Eq. (17).

$$X_{\text{cool}} = (T_{\text{Al}} > T_{\text{cool}} + T_{\text{f}}) + (T_{\text{Al}} < T_{\text{cool}} + T_{\text{f}}) \cdot (T_{\text{Al}} > T_{\text{cool}}) \cdot \left(\frac{dT_{\text{Al}}}{dt} < 0\right) \quad (17)$$

Finally, the control system during the cooling phase was modeled by adding Eq. (18) as an expression for the heat flux on the Peltier module contact face. The opposite value (*i.e.* positive) of this heat flux was applied to the heat sink to represent heat transfer through the Peltier module.

$$Q_{\text{cool}} = -X_{\text{cool}} \cdot Q_{\text{TEC}} \quad (18)$$

3.7 Simulating Convective Heat Loss

The convective heat loss from the heat sinks to the surrounding air was modeled through Eq. (19).

$$Q_{\text{conv}} = \frac{1}{2R_{\text{hs}}}(T_{\text{hs}} - T_{\infty}) \quad (19)$$

T_{hs} is the heat sink temperature derived within COMSOL through a domain point probe (located at point C in Fig. 6), T_{∞} is the ambient air temperature, and R_{hs} is the thermal resistance of the heat sink. When the cooling fans are inactive, the heat sink thermal resistance under natural convection, R_{n}, is 4.7 W/K [3]. When the cooling fans are active, the heat sink thermal resistance under forced convection, R_{f}, is 0.8 W/K [3].

During the cooling phase, the convective heat loss from the heat sink switches between natural and forced dependent upon the ON/OFF status of the fans. This was modeled through Eq. (20).

$$R_{\text{hs}} = R_{\text{n}} - (R_{\text{n}} - R_{\text{f}}) \cdot X_{\text{cool}} \quad (20)$$

3.8 Conduction through Peltier Module

The Peltier modules were not physically modeled in COMSOL as they possess complex internal geometry. The conductive heat rate through the Peltier modules however, was modeled according to Eq. (21).

$$Q_{\text{cond}} = \frac{kA_{\text{TEC}}}{t_{\text{TEC}}}\Delta T_{\text{TEC}} \quad (21)$$

A_{TEC} is the surface area of the Peltier module, t_{TEC} is the conduction length or the thickness of the Peltier module, and k is the thermal conductivity of the Peltier module which is approximated to be 1.6 W/m·K [4].

4. Simulation Results

4.1 Domain Point Probes in PCM Sample

Six domain point probes were placed on the top surface of the PCM sample to visualize phase change along the radial direction. The locations of these probes are shown in Fig. 9.

4.2 Heating Phase

The simulated melting of eicosane is shown in Fig. 10. The outer glass surface was heated to 90 °C (363 K) in approximately 3 min and this temperature was maintained with an allowable fluctuation of 2.5 °C. The center of the PCM sample exceeded its melting temperature in 5.4 min, indicating complete phase change.

Temperature distribution plots (of a cross section) at 100, 200, and 400 seconds of elapsed time are shown in Fig. 11.

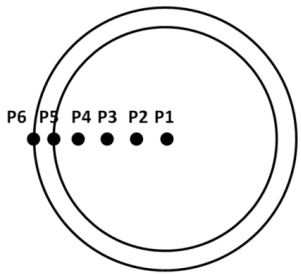

Figure 9 – Point probe locations on PCM sample and glass vial

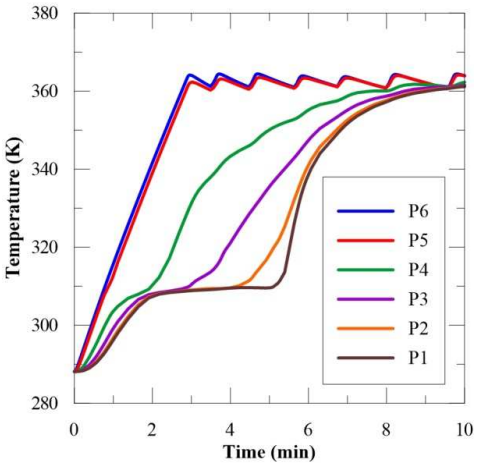

Figure 10 – Heating phase simulation with Eicosane

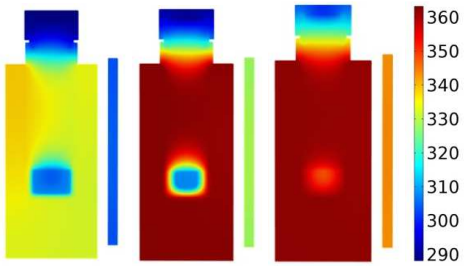

Figure 11 – Temperature distribution in Kelvin (K) at 100, 200 and 400 seconds of elapsed time

4.3 Cooling Phase

The simulated solidification of eicosane is shown in Fig. 12. The outer glass surface was cooled to 15 °C (288 K) in approximately 6 min and this temperature was maintained with an allowable fluctuation of 2.5 °C. The center of the PCM cooled below its freezing temperature in 10.9 min, indicating complete phase change.

5. Experimental Results Comparison

5.1 Heating Control System

The simulated and experimental aluminum housing temperatures in response to the heating control system are shown in Fig. 13. COMSOL accurately predicted the housing temperature with a maximum error of 10 % relative to the 75 °C temperature rise. This error is most likely associated with convective heat loss through the aluminum housing walls which was neglected in COMSOL simulations.

5.2 Cooling Control System

The simulated and experimental aluminum housing temperatures in response to the cooling control system are shown in Fig. 14. Similar to the heating phase, COMSOL accurately predicted the behavior of the Peltier modules with a maximum error of 10 % relative to the 75 °C temperature drop. This error is primarily associated with limitations in predicting the non-linear behavior of Peltier modules.

5.3 Duration of Fusion

The simulated and experimental phase change durations for melting are listed in Table 4; the corresponding simulation times are also included. COMSOL predicted an additional melting time of approximately 2 min for all PCM samples; this corresponds to relative errors ranging from 50 % to 80 % depending on the experimental melt time.

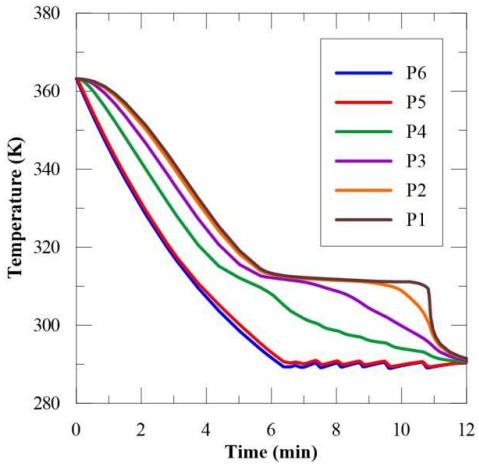

Figure 12 – Cooling phase simulation with Eicosane

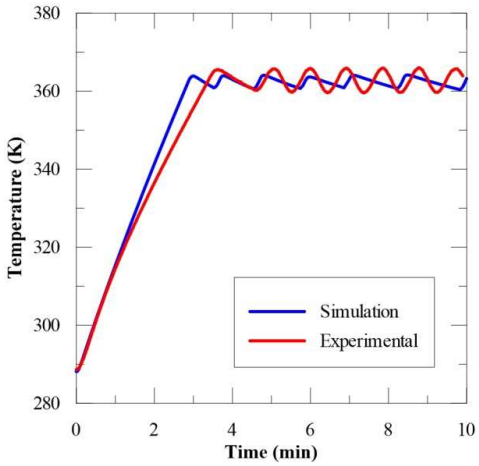

Figure 13 – Comparison of simulated and experimental aluminum housing temperatures during the heating phase

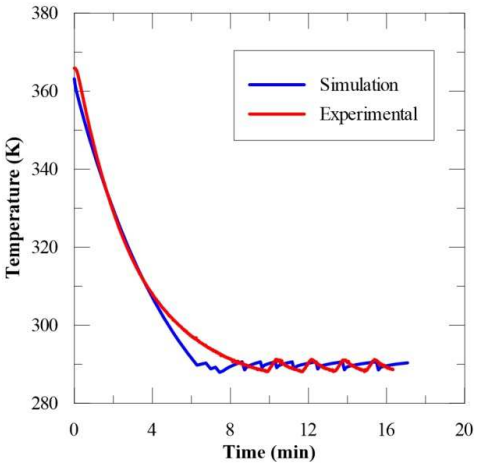

Figure 14 – Comparison of simulated and experimental aluminum housing temperatures during the cooling phase

This error was primarily associated with the dynamic behavior of the solid-liquid PCM mixture. Since fusion initiates at the side and bottom faces of the PCM samples, the remaining portion of solid PCM at the center eventually sinks and melts at a faster rate than that predicted by COMSOL. Additionally, free convection within the melted PCM samples results in higher heat transfer rates and hence, faster melting. From a design perspective, neglecting these dynamic behaviors resulted in a conservative prediction.

5.4 Duration of Solidification

The simulated and experimental phase change durations for solidification are listed in Table 5. COMSOL accurately predicted phase change durations with a maximum relative error of 9 %. This improvement in accuracy relative to the melting simulations was expected as the solid-liquid dynamics are less effected during solidification. The existing error was associated with inaccuracies in Eq. (1) and Eq. (3), as well as with limitations in predicting the behavior of Peltier modules.

Table 4 – Simulated and experimental durations for PCM melting

PCM	Eicosane	Docosane	Myristic Acid
Experimental	~ 3 min	~ 4 min	~ 5 min
COMSOL	5.4 min	6.3 min	7.5 min
% Error	80 %	58 %	50 %
Sim. Time	54.7 min	74.3 min	52.6 min

Table 5 – Simulated and experimental durations for PCM solidification

PCM	Eicosane	Docosane	Myristic Acid
Experimental	~ 10 min	~ 9 min	~ 8 min
COMSOL	10.9 min	9.6 min	8.3 min
Relative Error	9 %	6.6 %	3.8 %
Sim. Time	19.5 min	79.8 min	23.5 min

6. Conclusions

COMSOL Multiphysics was successfully used to validate the design of the thermal cycling system. Simulations showed that the selected cartridge heaters and thermoelectric cooling assemblies would regulate the housing temperature and induce phase change within a practical timeframe.

Additionally, complex behaviors including phase change, thermoelectric cooling, and temperature control were successfully modeled in COMSOL using only the Heat Transfer in Solids physics node. Upon comparison with experimental data, the methods used were deemed to produce favorable results.

References

1. Cabeza, L. F., Marin, J. M., Mehling, H., & Zalba, B. Review on thermal energy storage with phase change: materials, heat transfer analysis and applications. *Applied Thermal Engineering*, **V. 23**, P. 251-283. (2002).

2. VT-199-1.4-0.8 Thermoelectric Module Specifications. *TE Technology*. P. 2. (2010).

3. Kheirabadi, A. C., Groulx, D. Design of an Automated Thermal Cycler for Phase Change Material Phase Transition Stability Studies. *LAMTE*, P. 43 – 44. (2014).

4. Thermoelectric Handbook. *Laird Technologies*. P. 13. (2010).

5. Yaws, C. L. Yaws' Critical Property Data for Chemical Engineers and Chemists. *Knovel*. (2014).

Acknowledgements

The authors would like to thank the Natural Science and Engineering Research Council of Canada (NSERC), the Canadian Foundation for Innovation (CFI) and Intel Corporation for their financial contribution to this work.